Joachim Brossmann, MD[2] • Klaus-Werner Preidler, MD • Bénedicte Daenen, MD
Robert A. Pedowitz, MD, PhD • Reimer Andresen, MD • Paul Clopton, MS
Debra Trudell, RA • Mini Pathria, MD • Donald Resnick, MD

Imaging of Osseous and Cartilaginous Intraarticular Bodies in the Knee: Comparison of MR Imaging and MR Arthrography with CT and CT Arthrography in Cadavers[1]

PURPOSE: To compare magnetic resonance (MR) imaging and MR arthrography with computed tomography (CT) and CT arthrography in the detection of intraarticular bodies in the knee.

MATERIALS AND METHODS: Cuboid (3- or 6-mm-long sides) osseous and cartilaginous bodies were implanted in 16 cadaveric knee specimens. MR imaging was performed with T1-weighted spin-echo (SE), T2-weighted SE, proton-density–weighted SE, gradient recalled acquisition in the steady state (GRASS), and spoiled GRASS sequences. MR arthrography was performed in two phases with saline and 2 mmol/L gadopentetate dimeglumine. CT and CT arthrography were performed in the transaxial plane.

RESULTS: MR arthrography yielded the highest accuracy for the detection of osseous and cartilaginous bodies combined (92%) and was significantly ($P < .01$) better than MR imaging (57%–70%), CT arthrography (80%), and CT (74%). Accuracy of CT arthrography was significantly better than that of MR imaging and that of CT. Accuracy of saline-enhanced MR arthrography was significantly inferior ($P < .001$) to that of gadolinium-enhanced MR arthrography.

CONCLUSION: MR arthrography is the best imaging technique for detection of individual intraarticular bodies. CT arthrography is the second most accurate method. Spoiled GRASS and T2-weighted SE sequences are the most accurate at MR imaging. The presence of intraarticular fluid and performance of saline-enhanced MR arthrography improve detectability of intraarticular bodies.

INTRAARTICULAR bodies in joints are a common clinical finding and may provoke clinical complaints (pain, swelling, locking) that necessitate surgical intervention (1). Such bodies may consist of bone, cartilage, or both, or, rarely, they may be composed of fibrous tissue, unorganized fibrin, fat, or blood, or they may represent foreign bodies (2–4). Although intraarticular bodies may be encountered in virtually any joint, the knee is affected most often.

Imaging is usually necessary to confirm the clinical diagnosis and to localize the intraarticular bodies prior to surgery, as intraarticular bodies may be missed during arthroscopy (1). Radiography and conventional tomography are useful only when radiopaque intraarticular bodies are present. Performance of conventional arthrography and arthrotomography with single- or double-contrast technique have been suggested, especially in cases of radiolucent intraarticular bodies (5–7). Computed tomography (CT) and CT arthrography with single- or double-contrast technique have been employed successfully in this clinical situation and are considered the imaging methods of choice (8–12). Ultrasonography (US) also has been employed for the diagnosis of intraarticular bodies (13).

Magnetic resonance (MR) imaging is widely accepted as the imaging technique of choice in a variety of musculoskeletal disorders and internal derangements of joints. MR arthrography has been performed successfully to improve diagnosis of various pathologic conditions of joints (eg, cartilage disorders and osteochondritis dissecans) (14–21). Although the usefulness of MR imaging for the diagnosis of intraarticular bodies has been described (15,22,23), no definitive studies have been reported, to our knowledge, on the application of MR imaging and MR arthrography to the detection of intraarticular bodies.

The purpose of this study was to compare MR imaging, MR arthrography, CT, and CT arthrography in the diagnosis of individual osseous and cartilaginous intraarticular bodies in cadaveric knee specimens.

MATERIALS AND METHODS

A total of 48 cartilaginous and 49 osseous bodies were created experimentally from fresh patellae specimens. For each type, cuboid bodies were created (3-mm-long sides [26 cartilaginous, 26 osseous] and 6-mm-long sides [22 cartilaginous, 23 osseous]). All cartilaginous bodies were examined radiographically to exclude calcific or osseous components. The bodies

Index terms: Computed tomography (CT), comparative studies, 452.12111, 452.12141 • Knee, arthrography, 452.12111, 452.12141, 452.121412 • Knee, CT, 452.12111 • Knee, MR, 452.12141, 452.121412 • Magnetic resonance (MR), comparative studies, 452.12111, 452.12141

Abbreviations: GRASS = gradient recalled acquisition in the steady state, PD = proton-density, SE = spin-echo.

Radiology 1996; 200:509–517

[1] From the Departments of Radiology (J.B., K.W.P., B.D., R.A., D.T., M.P., D.R.), Orthopedic Surgery (R.A.P.), and Research (P.C.), Veterans Administration Medical Center, 3350 La Jolla Village Dr, San Diego, CA 92161. From the 1995 RSNA scientific assembly. Received January 11, 1996; revision requested February 26; revision received March 11; accepted March 20. Supported in part by Veterans Administration grant SA360 and Deutsche Forschungsgemeinschaft grant BR 1499. **Address reprint requests to** D.R.
[2] Current address: Department of Radiology, Klinik für Radiologische Diagnostik, Kiel, Germany.
© RSNA, 1996

then were implanted into a total of 16 fresh cadaveric knee specimens (nine female, seven male; age range at death, 66–85 years). The knees were opened surgically along the medial aspect of the patella, and the bodies were sutured (Prolene 5-0; Ethicon, Somerville, NJ) to specific locations in the joint. For each type of intraarticular body, four knee specimens were used.

Six locations were possible for placement of the intraarticular bodies in the suprapatellar pouch, including the medial and lateral gutters, and four locations were possible in the intercondylar region and the posterior joint space (Fig 1) (total, 56 locations). The number of bodies in each location ranged from 0 to the maximum number possible. The distribution and number of bodies implanted was based on logical reasoning, so that approximately the same number of bodies of each size and type were available for evaluation in identical locations (Table 1). A 7-F vascular sheath was introduced percutaneously into the suprapatellar pouch to allow later instillation of gadopentetate dimeglumine (Magnevist; Schering, Berlin, Germany) or air for MR arthrography or CT arthrography, respectively. The knee joints then were closed surgically while submerged in water, to prevent air inclusions. Prior to imaging, residual water in the knee joint was removed as completely as possible by means of aspiration.

Table 1
Anatomic Distribution of Types of Implanted Intraarticular Bodies in 16 Knee Specimens

Body Type	Length of Side (mm)	Suprapatellar Pouch, Lateral and Medial Gutters (n = 24)	Intercondylar Region (n = 16)	Posterior Joint Space (n = 16)	Total (n = 56)
Bone	3	10	8	8	26
Bone	6	11	8	4	23
Cartilage	3	10	8	8	26
Cartilage	6	9	8	5	22

Note.—Numbers are number of bodies placed per location.

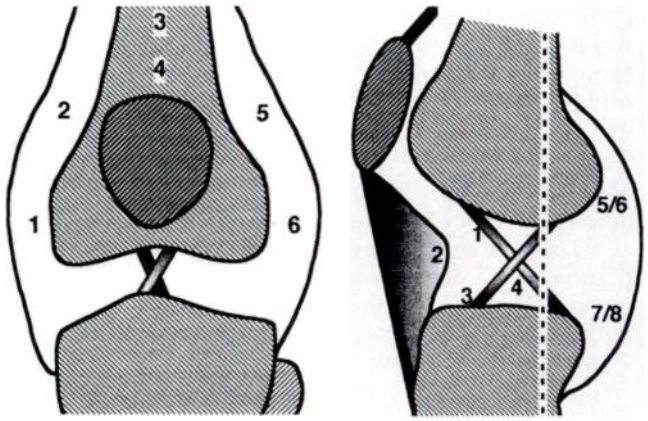

a. b.

Figure 1. Schematic display of the possible locations of the intraarticular bodies. **(a)** Six locations in the suprapatellar pouch and medial and lateral gutter and **(b)** four locations in the intercondylar area: middle third of the anterior cruciate ligament (*1*), behind the Hoffa fat pad (*2*), attachment site of the anterior cruciate ligament to the tibial plateau (*3*), and the posterior cruciate ligament (*4*); and four locations in the posterior joint space above (*5*, *6*), and below (*7*, *8*) the joint line.

MR Imaging and MR Arthrography

All knees were examined with a 1.5-T superconducting imager (Signa; GE Medical Systems, Milwaukee, Wis). The knees were positioned supine in a specialized receive-only knee coil. Standard MR imaging sequences were employed: T2-weighted; proton-density (PD)-weighted; T1-weighted spin-echo (SE), T1-weighted two- and three-dimensional spoiled gradient recalled acquisition in the steady state (spoiled GRASS), and T2-weighted multiplanar GRASS images were acquired in the axial and sagittal planes. The MR imaging protocol is summarized in Table 2. To determine the usefulness of saline-enhanced MR imaging and the effects of intraarticular fluid to simulate a joint effusion, 40 mL saline was injected in the knee joints and MR imaging was repeated as before. Then, the saline was evacuated from the knee and 40 mL of a 2 mmol/L gadopentetate dimeglumine solution (Magnevist [1 mL in 250 mL saline]; Schering, Berlin Germany) was injected through the sheath, following the protocol described by Engel (24). Gadolinium-enhanced MR arthrography was accomplished with T1-weighted SE imaging in the axial and sagittal planes.

CT and Single-Contrast CT Arthrography

After MR imaging, all fluid was aspirated from the knee joints, and CT was performed in the transaxial plane (Tomoscan 60 TX; Philips, Best, The Netherlands). Contiguous 3-mm-thick sections (312 × 312 matrix, 120 kV, 300 mA) were obtained that covered the complete joint cavity. After insufflation of 40 mL air, the knees were rescanned in the prone position, which allowed better distribution of air in the posterior and intercondylar regions of the joint, with use of the same imaging parameters. Images were obtained with narrow and wide window settings for best display of the soft tissues and bones.

Evaluation and Statistical Analysis

All images were evaluated by two readers (K.W.P., B.D.) who were experienced in musculoskeletal radiology. The readers were blinded with regard to information about the number, size, location, and type of intraarticular bodies, and they did not have access to all of the imaging examinations of a single knee. All images obtained with the different MR and CT techniques of all knees were provided in a randomized fashion. Diagnosis of an intraarticular body was reached by consensus. The location of the bodies was marked on the images, and all images then were reviewed simultaneously by two other investigators (J.B., R.A.P.), who were familiar with the location, size, and type of the bodies. These investigators reviewed the images obtained with all MR and CT techniques simultaneously to determine true-positive, true-negative, false-positive, and false-negative diagnoses for each individual body as depicted with each imaging technique. Sensitivity, specificity, and accuracy of each imaging technique were determined. To evaluate the suitability of each technique for detection of the bodies, only transaxial images were considered. The significance of these comparative results was assessed with the McNemar sign test (25).

RESULTS

Diagnostic sensitivity and accuracy were better for larger bodies (Table 3). Sample sizes for sensitivity, specificity, and accuracy regarding the intraarticular bodies (3- and 6-mm-long sides) with the different imaging techniques were too small for a statistically valid analysis. The results for the combination of osseous (Fig 2) and

Table 2
MR Imaging Sequences

Modality and Sequence	Imaging Plane	Section Thickness (mm)	Intersection Gap (mm)	Repetition Time (msec)	Echo Time (msec)	Flip Angle*	Number of Signals Acquired	Matrix Size (pixel)	Field of View (cm)
MR imaging									
Fast SE PD-weighted (localizer)	Coronal	4.0	1	3,000	19	NA	2	256 × 256	14
T2-weighted SE	Sagittal	4.0	1	2,200	90	NA	2	192 × 256	14
PD-weighted SE	Sagittal	4.0	1	2,200	20	NA	2	192 × 256	14
Three-dimensional spoiled GRASS	Sagittal	1.5	0	52	10	60	2	128 × 256	14
T2-weighted SE	Axial	4.0	1	2,200	90	NA	2	192 × 256	14
PD-weighted SE	Axial	4.0	1	2,200	20	NA	2	192 × 256	14
Two-dimensional spoiled GRASS	Axial	4.0	1	52	10	60	2	128 × 256	14
GRASS	Axial	4.0	1	400	19	20	2	192 × 256	14
T1-weighted SE	Axial	4.0	1	500	20	NA	2	192 × 256	14
MR arthrography	Axial, sagittal	4.0	1	500	20	NA	2	192 × 256	14

* NA = not applicable.

Table 3
Sensitivity, Specificity, and Accuracy for Osseous and Cartilaginous Bodies Separately

Modality and Sequence	Osseous Body (by length of side [mm])						Cartilaginous Body (by length of side [mm])					
	3 (n = 26)			6 (n = 23)			3 (n = 26)			6 (n = 22)		
	Sensitivity	Specificity	Accuracy	Sensitivity	Specificity	Accuracy	Sensitivity	Specificity	Accuracy	Sensitivity	Specificity	Accuracy
MR imaging												
PD-weighted SE	42.3	96.7	71.4	69.6	90.9	82.1	7.7	80.0	46.4	50.0	94.1	76.8
T2-weighted SE	53.8	86.7	71.4	69.6	84.8	78.6	11.5	66.7	41.1	77.3	82.4	80.4
GRASS	69.2	80.0	75.0	73.9	78.8	76.8	0.0	63.3	33.9	4.5	64.7	41.1
Spoiled GRASS	76.9	76.7	76.8	82.6	87.9	85.7	34.6	80.0	58.9	50.0	55.9	53.6
T1-weighted SE	50.0	96.7	75.0	73.9	87.9	82.1	11.5	96.7	57.1	36.4	82.4	64.3
Gadolinium-enhanced MR arthrography	88.5	96.7	92.9	91.3	97.0	94.6	80.8	93.3	87.5	81.8	97.1	91.1
CT	92.3	86.7	89.3	100.0	93.9	96.4	3.8	80.0	44.6	31.8	85.3	64.3
CT arthrography	96.2	90.0	92.9	100.0	93.9	96.4	23.1	83.3	55.4	54.5	91.2	76.8

Note.—Numbers are percentages.

cartilaginous (Figs 3, 4) bodies, as well as the results of the combined evaluation of all bodies (osseous and cartilaginous bodies of all sizes) are shown in more detail (Table 4, Figs 5–7). These results more closely simulate the clinical situation, in which the bodies vary in size and are of unknown type.

Osseous Bodies

The most sensitive MR techniques for the detection of osseous bodies were MR arthrography (90%) and spoiled GRASS imaging (80%) (Tables 3, 4; Fig 5). The sensitivity of each was significantly better than that of GRASS, T1-weighted SE, T2-weighted SE, and PD-weighted SE imaging ($P < .01$). The osseous bodies were best seen on MR arthrograms and spoiled GRASS and GRASS images as structures with low signal intensity (Fig 2). Susceptibility effects helped delineate the osseous bodies to better advantage on spoiled GRASS and GRASS images. T1-weighted SE, T2-weighted SE, and PD-weighted SE images showed the least contrast between the bodies and the surrounding tissues. Arthrographic effects of residual joint fluid helped delineate the osseous bodies on T2-weighted SE and GRASS images (Fig 2).

Osseous bodies were depicted with both CT and CT arthrography with the same sensitivity (96% and 98%, respectively). CT and CT arthrography were significantly more sensitive in the depiction of osseous bodies than spoiled GRASS, GRASS, and T2-weighted SE imaging ($P < .05$). No significant differences were found in sensitivity between CT and MR arthrography ($P = .38$) and between CT arthrography and MR arthrography ($P = .13$).

Cartilaginous Bodies

The most sensitive MR technique for the detection of cartilaginous bodies was MR arthrography, with 81% sensitivity (Fig 3). Gadolinium-enhanced MR arthrography was significantly more accurate ($P < .01$) in the depiction of cartilaginous bodies than MR imaging with all sequences (Tables 3, 4; Fig 6). Sensitivities of T2-weighted

SE and spoiled GRASS sequences for the detection of cartilaginous bodies were significantly greater than sensitivities of PD-weighted SE ($P < .04$ and $P < .05$, respectively), T1-weighted SE ($P = .004$ and $P = .01$, respectively), and GRASS ($P < .0001$ and $P < .0001$, respectively) imaging. Sensitivities of PD-weighted SE and T1-weighted SE imaging were significantly greater than sensitivity of GRASS imaging ($P < .0001$ and $P = .002$, respectively). Cartilaginous bodies were depicted with low signal intensity at MR arthrography; with intermediate signal intensity at T2-weighted SE, T1-weighted SE, and PD-weighted SE imaging; and with high signal intensity at spoiled GRASS and GRASS imaging (Fig 3). Arthrographic effects at T2-weighted SE imaging again helped detection of cartilaginous bodies. No such effect was seen at T2-weighted GRASS imaging, however, when cartilage was depicted with the same high signal intensity as residual joint fluid.

In the detection of cartilaginous bodies, CT arthrography was significantly better than CT (38% versus 17%, $P = .002$ [Table 4, Fig 6]). Cartilaginous bodies had attenuation similar to that of the surrounding soft tissues and were difficult to delineate at CT (Fig 4). The sensitivity of CT arthrography was not statistically different from that of spoiled GRASS, T2-weighted SE, PD-weighted SE, and T1-weighted SE imaging ($P > .12$). CT arthrography, however, was significantly more sensitive than GRASS imaging ($P < .04$) in the detection of cartilaginous bodies. The sensitivity of MR arthrography was significantly greater than that of CT, CT arthrography, and MR imaging with all sequences ($P = .0001$) in the detection of cartilaginous bodies.

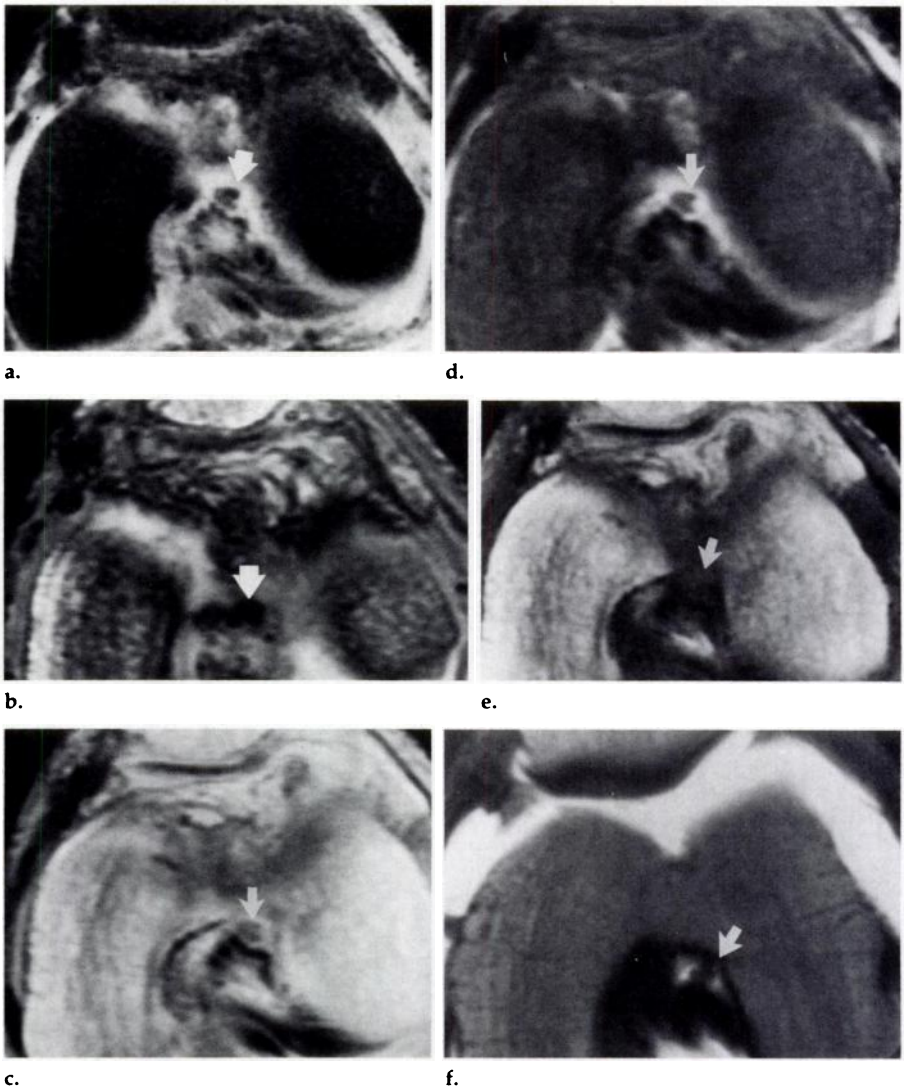

Figure 2. Transaxial MR imaging of a cuboid (3-mm-long sides) osseous body (arrow). The body is clearly depicted on the **(a)** T2-weighted GRASS (repetition time msec/echo time msec = 400/19, with 20° flip angle) image and **(b)** the T1-weighted spoiled GRASS (52/10, with 60° flip angle) image as a structure with low signal intensity. **(c)** The body is not depicted as clearly on the PD-weighted SE (2,200/20) image. **(d)** The body is clearly depicted on the T2-weighted SE (2,200/90) image, owing to arthrographic effects of a small joint effusion. **(e)** The body is not depicted as clearly on the T1-weighted SE (500/20) image, and the body was missed at review. **(f)** The body is clearly depicted on the gadolinium-enhanced T1-weighted SE (500/20) MR arthrogram.

Osseous and Cartilaginous Bodies

For the evaluation of all bodies (osseous and cartilaginous, all sizes) MR arthrography yielded the greatest sensitivity (86%) and was significantly more sensitive than MR imaging with all sequences ($P < .01$ [Table 5, Fig 7]). With MR imaging, the second greatest sensitivity was found with spoiled GRASS imaging (61%), which was significantly greater than that of T1-weighted SE, PD-weighted SE, and GRASS imaging ($P < .01$). The sequence with overall poorest results for the detection of osseous and cartilaginous bodies was GRASS (sensitivity, 37%).

Sensitivity for the detection of all osseous and cartilaginous bodies of all sizes was significantly greater with CT arthrography (68%) than with CT (57%) ($P = .001$); however, sensitivities of both CT and CT arthrography were significantly less than sensitivity of MR arthrography (86%) ($P < .002$ [Fig 7]). Although the sensitivity of CT arthrography was not statistically different ($P = .23$) from that of spoiled GRASS in the detection of all bodies, it was significantly greater than that of the other nonenhanced MR imaging sequences ($P < .006$). The sensitivity of CT was not statistically different from that of spoiled GRASS or T2-weighted SE imaging ($P > .48$) but was greater than that of T1-weighted SE, PD-weighted SE, or GRASS imaging ($P < .02$).

The specificities of MR arthrography and T1-weighted SE and PD-weighted SE imaging and CT arthrography were not statistically different ($P > .07$), but they were significantly greater ($P < .01$) than those of spoiled GRASS, T2-weighted SE, and GRASS imaging (Fig 7). The specificity of CT was significantly greater than that of spoiled GRASS, T2-weighted SE, or GRASS imaging ($P < .02$) but was statistically inferior to that of MR arthrography ($P < .02$).

MR arthrography was significantly more accurate than all other imaging modalities ($P = .0001$ [Table 4]). CT arthrography yielded the second

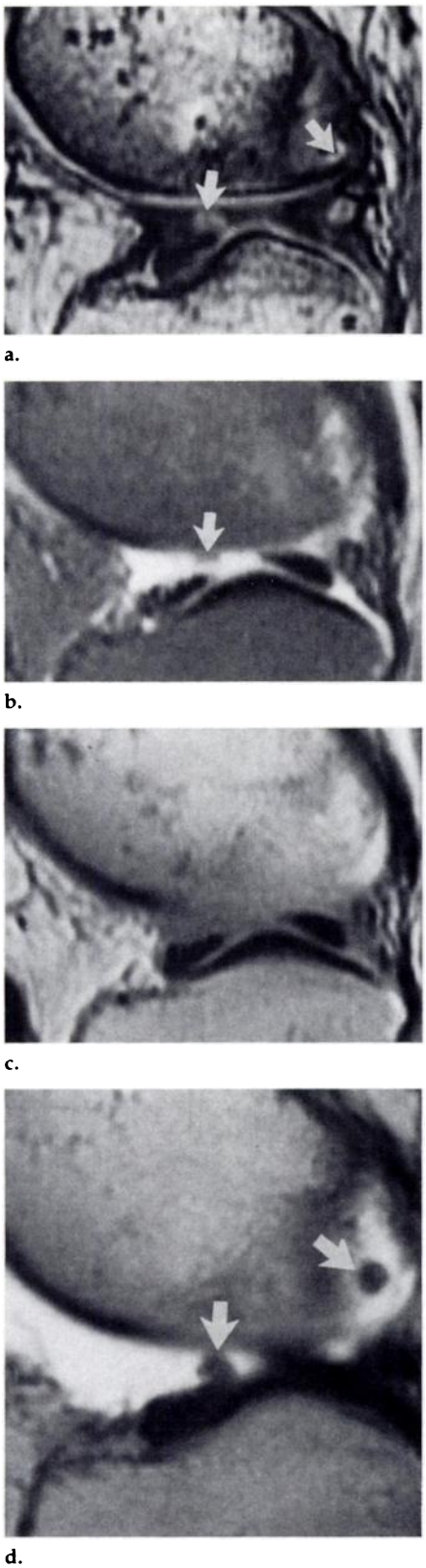

Figure 3. MR imaging in two cuboid cartilaginous bodies (3-mm-long sides) (arrows) in the sagittal plane. **(a)** The bodies are depicted on the T1-weighted spoiled GRASS (52/10, with 60° flip angle) image as structures with high signal intensity. **(b)** Only the anterior body is depicted on the T2-weighted SE (2,200/90) image, which is enhanced by the arthrographic effect of a small joint effusion. **(c)** None of the bodies are depicted on the PD-weighted SE (2,200/20) image. **(d)** The bodies are most clearly depicted, with low signal intensity, on the gadolinium-enhanced T1-weighted SE (500/20) MR arthrogram.

highest accuracy, which was significantly greater than that of spoiled GRASS, PD-weighted SE, T2-weighted SE, T1-weighted SE, GRASS imaging, or CT ($P < .002$). The accuracies of spoiled GRASS, PD-weighted SE, T2-weighted SE, T1-weighted SE imaging, or CT were not statistically different from each other ($P > .18$). The accuracy of CT, however, was greater than that of GRASS imaging ($P < .001$).

Effect of Intraarticular Saline on the Detection of Intraarticular Bodies with MR Imaging

Overall, accuracy for the detection of osseous and cartilaginous bodies combined improved with the injection of saline compared with nonenhanced imaging (Table 4). Saline-enhanced MR imaging was superior to nonenhanced MR imaging with spoiled GRASS ($P < .001$), GRASS ($P < .001$), PD-weighted SE ($P < .01$), and T2-weighted SE ($P < .001$) sequences but yielded no advantage compared with nonenhanced MR imaging with the T1-weighted SE sequence ($P = .99$). Despite the improved detection of intraarticular bodies at saline-enhanced MR imaging, however, the accuracy of gadolinium-enhanced MR arthrography was superior for the detection for all types of intraarticular bodies ($P < .001$).

The improved accuracies for saline-enhanced MR arthrography compared with nonenhanced MR imaging were mainly related to improved sensitivities for the detection of osseous and cartilaginous bodies at MR imaging with all sequences. However, significantly greater sensitivities for saline-enhanced MR arthrography were found for the detection of cartilaginous bodies only with GRASS ($P < .001$) and T2-weighted SE sequences ($P < .001$) and for the detection of osseous bodies only with the T2-weighted SE sequence ($P = .04$). Although the specificities for the detection of osseous and cartilaginous bodies combined also improved for saline-enhanced MR arthrography with all sequences, this effect was statistically significant only with spoiled GRASS ($P < .001$) and T2-weighted SE sequences compared with nonenhanced MR imaging ($P < .001$).

Sagittal versus Transaxial MR Imaging

To determine the best imaging plane for evaluation of the intercondylar area and posterior joint space in the knee, results of spoiled GRASS, PD-weighted SE, T2-weighted SE imaging, and MR arthrography were compared in the axial and sagittal planes. Significantly greater accuracies were achieved with spoiled GRASS, T2-weighted SE, and PD-weighted SE imaging in the sagittal plane (81%, 53%, and 49%, respectively) compared with the transaxial plane (58%, 46%, and 28%, respectively [$P < .04$]). No significant differences were found at MR arthrography between the transaxial and sagittal planes (75% and 70%, respectively [$P > .05$]).

DISCUSSION

The usefulness of MR imaging in the diagnosis of internal derangements of joints is widely accepted. Similarly, the importance of MR imaging and MR arthrography for the diagnosis of osteochondritis dissecans (16,21,24,26), cartilage defects (18,24,27), and other internal derangements of joints (14–7,19,20,23,24,28,29) has been well demonstrated. Only a few reports, however, comment on the usefulness of MR imaging and MR arthrography in the diagnosis of intraarticular bodies (15,22,23,29), and MR imaging is not considered the primary imaging method in this clinical situation.

Intraarticular bodies can be identified at radiography and conventional tomography when they are radiopaque, but in the knee they may be difficult to discriminate from central osteophytes, meniscal ossification, calcification, sesamoid bones, and prominent tibial spines (7,8,30). Conventional arthrography and arthrotomography with single- or double-contrast technique facilitate the diagnosis of radiolucent fragments (5,7).

CT and CT arthrography provide thin-section images of regions of complex anatomy with good soft-tissue contrast and no superimposition of structures. These techniques have been employed successfully in various joints (8–12). Limitations of CT, however, include restriction to one imaging plane, especially in complex anatomic regions, and difficulties in discriminating between cartilage, intraarticular fibrinoid structures (as in rheumatoid arthritis), and adjacent soft tissue (11). Use of multiplanar CT reformations has improved diagnostic accuracy (8) and has helped exclude possible pitfalls (eg, osteophytes and

bone prominences that simulate intraarticular bodies) (8,30). Single-contrast CT arthrography technique with air has improved the diagnostic yield in cases of osteochondritis dissecans and the ability to discriminate capsular calcifications (8,11,12), and it has been reported to allow identification of osseous and osteocartilaginous bodies as small as 2–3 mm in diameter (8,11). Additional application of a positive contrast agent has not contributed to improved diagnostic accuracy. Indeed, the use of a positive contrast agent may obscure small bodies (11). US also has been used for the diagnosis of intraarticular bodies (13). Detectability of abnormalities depends on the presence of intraarticular fluid and acoustic shadowing, which is present only if the intraarticular bodies are ossified or calcified; otherwise, intraarticular bodies may be missed.

Murphy (22) found results with MR imaging are moderately good in detection of intraarticular bodies. In a comparative study of double-contrast CT arthrography and nonenhanced MR imaging of the shoulder, Jahnke et al (15) found that MR imaging and CT arthrography had the same diagnostic accuracy in the diagnosis of intraarticular bodies (sensitivity for both techniques, 50%; specificity for MR imaging, 95%, and for CT arthrography, 98%). In their study of 25 patients with shoulder complaints, however, intraarticular bodies were found in only two patients, and no information was given regarding the size or the type of the bodies. Similar data were provided by Neumann et al (29). Their study also was limited by the small number of intraarticular bodies ($n = 2$) that were examined. Superior display of intraarticular bodies with MR arthrography was mentioned by Chandnani et al (23), especially when the bodies were small. Improved diagnosis of intraarticular bodies with MR imaging was noted in the presence of fluid and the role of MR arthrography was emphasized as a useful method in the absence of fluid (31). To our knowledge, however, CT arthrography is still recommended generally for the diagnosis of intraarticular bodies.

On the basis of our results, MR arthrography seems to be the imaging method of choice in those situations in which neither the size nor the type of suspected intraarticular bodies are known. For combined evaluation of all osseous and cartilaginous bodies, MR arthrography yielded the best sensitivity and specificity, resulting in an accuracy of 92%. This was significantly better than that for MR imaging with all sequences, CT arthrography, and CT. Although CT arthrography was significantly better than nonenhanced MR imaging, CT was equivalent to these MR imaging sequences.

The sensitivities of CT and CT arthrography were superior to those of nonenhanced MR imaging for the diagnosis of osseous bodies in the knee, but neither CT nor CT arthrography were significantly more sensitive than gadolinium-enhanced MR arthrography. Gradient-echo images (spoiled GRASS, GRASS) yielded the best sensitivities among the nonenhanced MR imaging sequences for the detection of osseous bodies; this finding agrees with the conclusion of Murphy (22). The sensitivity of gradient-echo imaging to local susceptibility distortions around the intraarticular bodies is presumably an important factor in the superior results with these sequences in the diagnosis of osseous bodies; however, this effect also explains the lower specificity.

Dramatic differences between MR arthrography and MR imaging with all sequences were seen for diagnosis of cartilaginous bodies. Results with gadolinium-enhanced MR arthrography were significantly better than those with nonenhanced MR imaging with all sequences, CT arthrography, and CT, yielding a sensitivity of 81%. The sensitivity of CT arthrography (38%) for the detection of cartilaginous bodies was equivalent to that of spoiled GRASS and T2-weighted imaging; however, CT arthrography provided better specificity. The low sensitivity of CT arthrography for the detection of cartilaginous bodies is somewhat surprising and is explained primarily by inadequate distribution of air in the joint and also by the inability to differentiate the attenuation of cartilaginous bodies from that of adjacent soft tissues. PD-weighted SE, T1-weighted SE, and especially GRASS imaging were not suitable for the detection of cartilaginous bodies. CT arthrography was significantly better than CT for the detection of cartilaginous bodies.

Our results confirm those in previous reports that indicate saline-enhanced MR arthrography is feasible and advantageous (28,32). Improved accuracy for the detection of osseous and cartilaginous bodies was found at saline-enhanced MR imaging with all but T1-weighted SE sequences. The greatest effects of saline enhancement on sensitivity were noted for the T2-weighted SE and GRASS sequences, and on specificity were noted for the spoiled GRASS sequence. Diagnostic accuracy for the detection of osseous and cartilaginous bodies combined, however, was still significantly better for gadolinium-enhanced MR arthrography.

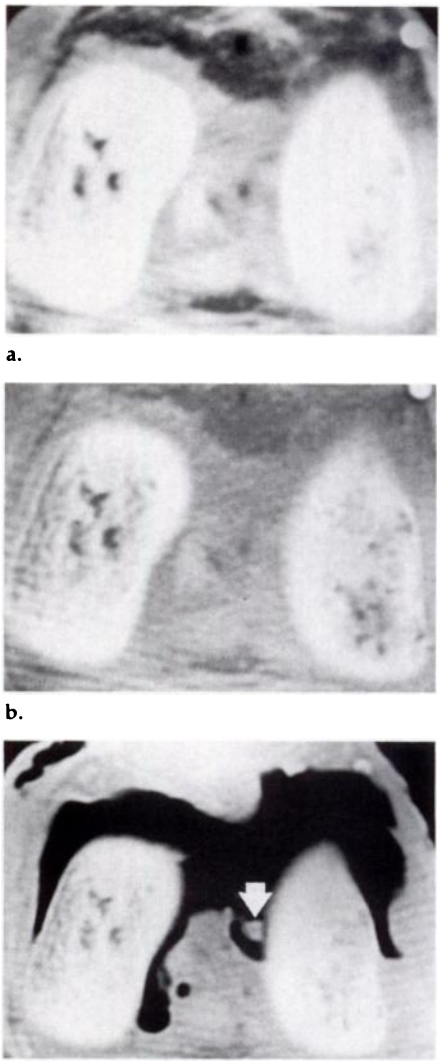

Figure 4. Transaxial CT scans of a cuboid cartilaginous body (3-mm-long sides) (arrow) in the intercondylar region. The body was not depicted on CT scans obtained with **(a)** narrow windows (level, 40 HU; width, 550 HU) or **(b)** wide windows (level, 500 HU; width, 2,400 HU). **(c)** The body was most clearly depicted on CT arthrogram obtained with wide window settings (level, 500 HU; width, 2,400 HU).

In the special situation of the knee, sagittal imaging is favored over axial imaging when the presence of intraarticular bodies is suspected in the intercondylar and posterior joint space. This may relate primarily to superior display of the anatomy and better delineation of the bodies adjacent to the tibial plateau in sagittal images. With the spoiled GRASS sequence, increased accuracy with sagittal images is also a result of 1.5-mm-thick sections com-

Table 4
Sensitivity, Specificity, and Accuracy for All Osseous and Cartilaginous Bodies

Modality and Sequence	All Osseous Bodies (n = 49)						All Cartilaginous Bodies (n = 48)						All Bodies (n = 97)					
	Sensitivity		Specificity		Accuracy		Sensitivity		Specificity		Accuracy		Sensitivity		Specificity		Accuracy	
	Other Modalities	Saline-enhanced MR Arthrography	Other Modalities	Saline-enhanced MR Arthrography	Other Modalities	Saline-enhanced MR Arthrography	Other Modalities	Saline-enhanced MR Arthrography	Other Modalities	Saline-enhanced MR Arthrography	Other Modalities	Saline-enhanced MR Arthrography	Other Modalities	Saline-enhanced MR Arthrography	Other Modalities	Saline-enhanced MR Arthrography	Other Modalities	Saline-enhanced MR Arthrography
MR imaging																		
PD-weighted SE	55.1	63.3	93.7	95.2	76.8	81.3	27.1	35.4	87.5	93.8	61.6	68.8	41.2	49.5	90.6	94.5	69.2	75.0
T2-weighted SE	61.2	75.5	85.7	90.5	75.0	83.9	41.7	68.8	75.0	89.1	60.7	80.4	51.5	72.2	80.3	89.8	67.9	82.1
GRASS	71.4	81.6	79.4	87.3	75.9	84.8	2.1	33.3	64.1	65.6	37.5	51.8	37.1	57.7	71.7	76.4	56.7	68.3
Spoiled GRASS	79.6	85.7	82.5	93.7	81.3	90.2	41.7	47.9	67.2	90.6	56.3	72.3	60.8	67.0	74.8	92.1	68.8	81.3
T1-weighted SE	61.2	63.3	92.1	90.5	78.6	78.6	22.9	31.3	89.1	84.4	60.7	61.6	42.3	47.4	90.6	87.4	69.6	70.1
Gadolinium-enhanced MR arthrography	89.8	NA	96.8	NA	93.8	NA	81.3	NA	95.3	NA	89.3	NA	85.6	NA	96.1	NA	91.5	NA
CT	95.9	NA	90.5	NA	92.9	NA	16.7	NA	82.8	NA	54.4	NA	56.7	NA	86.6	NA	73.7	NA
CT arthrography	98.0	NA	92.1	NA	94.6	NA	37.5	NA	87.5	NA	66.1	NA	68.0	NA	89.8	NA	80.4	NA

Note.—Numbers are percentages. NA = not applicable.

pared with the 4-mm-thick sections on transaxial images.

Some limitations apply to our study. First, the experimental situation may not reflect the clinical situation. For practical reasons, the intraarticular bodies were designed as cuboid shapes. This shape certainly is not physiologic and may have influenced the results. Such bodies were easy to create, however, and should not influence the signal intensities observed on the different MR images.

Second, the distribution of the bodies in our study may not reflect the physiologic situation; however, common locations for intraarticular bodies in the knee are the suprapatellar pouch, the popliteus tunnel, recesses beneath the menisci, and the intercondylar notch (1).

Third, the length of each side of the cuboid bodies was restricted to 3 or 6 mm, and the bodies consisted of either cartilage or bone. In the clinical situation, however, bodies of all sizes occur and they are predominantly of mixed consistency. The diameter of most reported intraarticular bodies has been 2–8 mm (11). Smaller bodies (sides < 1.5 mm long) could not be prepared reliably with our experimental methods. The primary intraarticular body (nidus) may be composed of only bone or cartilage or it may be composed of both (2–4), but intraarticular bodies undergo certain changes with predominantly proliferative alterations characterized by juxtaposed osseous and cartilaginous layering. In a series of more than 200 intraarticular bodies in 119 patients, Milgram (3) reported secondary calcification in 91.6%, cartilaginous layering in 86.6%, and osseous layering in 79.8%.

Fourth, although residual water from surgery was carefully aspirated from the knee joints prior to MR imaging, small amounts remained in the joints, which may have affected the sensitivity and specificity of MR imaging with all sequences to a varying degree. In particular, results with the T2-weighted sequences may have improved as a result of this arthrographic effect. The saline-enhanced examinations, however, showed significantly better results than the nonenhanced MR examinations, which indicates that the effect of residual fluid was not important. Also, small amounts of intraarticular fluid are physiologic, and intraarticular fluid volume may be pronounced in the clinical situation of intraarticular bodies.

Fifth, susceptibility artifacts may have been produced as a result of small air inclusions, piercing of the

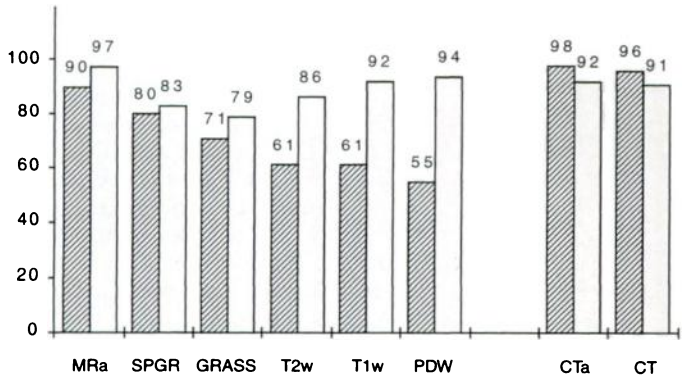

5.

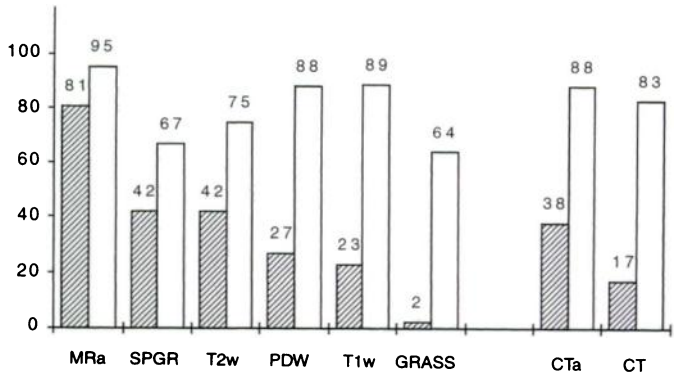

6.

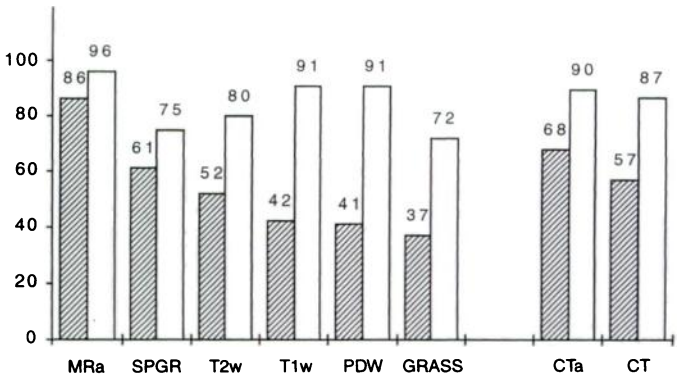

7.

Figures 5–7. Diagrammatic displays of sensitivity (lined box) and specificity (open box) of all nonenhanced MR imaging sequences, gadolinium-enhanced MR arthrography, CT, and CT arthrography for **(5)** all osseous bodies, **(6)** all cartilaginous bodies, and **(7)** combined osseous and cartilaginous bodies of all sizes. *CTa* = CT arthrography, *MRa* = MR arthrography, *PDW* = PD-weighted, *SPGR* = spoiled GRASS, *T1w* = T1-weighted, and *T2w* = T2-weighted.

bodies, and the suture material, which would produce false-positive results and improve visualization of the bodies. The suture material with the fewest susceptibility effects was chosen, however, and the effects were not prominent on the images.

Sixth, our study design does not represent the clinical imaging situation, in which images obtained with several different sequences and in several different imaging planes are evaluated simultaneously. Our study design was necessary, however, to allow determination of the best imaging sequences and planes to evaluate suspected intraarticular bodies. These sequences and planes may be added to the regular imaging protocol in such cases. Also, our results at CT may have been less successful than we would have achieved with state-of-the-art equipment.

In conclusion, this is the first study, to our knowledge, to compare simultaneously findings with MR imaging, MR arthrography, CT, and CT arthrography for the diagnosis of osseous and cartilaginous intraarticular bodies. Despite some experimental limitations, the results of this cadaveric study strongly suggest gadolinium-enhanced MR arthrography is the imaging method of choice to evaluate for suspected intraarticular bodies. Gadolinium-enhanced MR arthrography with T1-weighted SE should be the imaging method of choice regardless of the type of bodies present (which usually is not known in the clinical situation). If arthrography (CT or MR) is not planned or if the patient's consent cannot be obtained for arthrography, MR imaging with T1-weighted three-dimensional spoiled GRASS and T2-weighted SE sequences should be performed in at least two planes. The detection of intraarticular bodies was improved by intraarticular fluid at saline-enhanced MR arthrography, especially with T2-weighted SE and GRASS sequences, owing to the arthrographic effects. In cases of suspected intraarticular bodies in the knee, the intercondylar and posterior joint spaces should be examined preferably in the sagittal plane. On the basis of our results, CT arthrography should be the imaging method of choice if MR imaging is not available. Our conclusions are based on a cadaveric study with certain limitations, however, and our separate evaluation of imaging planes and MR imaging sequences was not performed as it would be clinically, when several imaging planes and sequences are evaluated simultaneously. Our results strongly support the need for clinical trials to evaluate MR imaging and MR arthrography in the diagnosis of intraarticular bodies. ■

References

1. Jonson LL. Arthroscopic surgery: principles and practice. 3rd ed. St Louis, Mo: Mosby, 1986; 669–787.
2. Milgram JW. The classification of loose bodies in human joints. Clin Orthop 1977; 124:282–291.
3. Milgram JW. The development of loose bodies in human joints. Clin Orthop 1977; 124:292–303.
4. Milgram JW, Rogers LF, Miller JW. Osteochondral fractures: mechanisms of injury and fate of fragments. AJR 1978; 130:651–658.
5. Staple TW. Extrameniscal lesions demonstrated by double-contrast arthrography of the knee. Radiology 1972; 102:311–319.
6. Thomas RH, Resnick D, Alazraki NP, Daniel D, Greenfield R. Compartmental evaluation of osteoarthritis of the knee: a comparative study of available diagnostic modalities. Radiology 1975; 116:585–594.
7. Resnick D. Arthrography, tenography, and bursography. In: Resnick D, ed. Diagnosis of bone and joint disorders. 3rd ed. Philadelphia, Pa: Saunders, 1995; 277–409.
8. Sartoris DJ, Kursunoglu S, Pineda C, Kerr R, Pate D, Resnick D. Detection of intraarticular osteochondral bodies in the knee using computed arthrotomography. Radiology 1985; 155:447–450.
9. Singson RD, Feldman F, Rosenberg ZS. Elbow joint: assessment with double-contrast CT-arthrography. Radiology 1986; 160:167–173.
10. Brody AS, Ball WS, Towbin RB. Computed arthrotomography as an adjunct to pediatric arthrography. Radiology 1989; 170:99–102.
11. Frahm R, Wimmer B. Suche nach freien gelenkkörpern im ellbogengelenk: konventionelle oder CT-arthrographie [Search for intraarticular loose bodies in the elbow joint: conventional or CT-arthrography [abstr in English]]. Radiologe 1990; 30: 113–115.
12. Holland P, Davies AM, Cassar-Pullicino VN. Computed tomographic arthrography in the assessment of osteochondritis dissecans of the elbow. Clin Radiol 1994; 49:231–235.
13. Van Holsbeeck M, Introcaso JH. Musculoskeletal ultrasound. St Louis, Mo: Mosby, 1991; 143–176.
14. Hodler J, Kursunoglu-Brahme SJ, Snyder

SJ, et al. Rotator cuff disease: assessment with MR arthrography versus standard MR imaging in 36 patients with arthroscopic confirmation. Radiology 1992; 182:431–436.
15. Jahnke AH, Petersen SA, Neumann C, Steinbach L, Morgan F. A prospective comparison of computerized arthrotomography and magnetic resonance imaging of the glenohumeral joint. Am J Sports Med 1992; 20:695–701.
16. Kramer J, Stiglbauer R, Engel A, Prayer L, Imhof H. MR contrast arthrography (MRa) in osteochondrosis dissecans. J Comput Assist Tomogr 1992; 16:254–260.
17. Applegate GR, Flannigan BD, Tolin BS, Fox JM, Del Pizzo W. MR diagnosis of recurrent tears in the knee: value of intraarticular contrast material. AJR 1993; 161:821–825.
18. Gagliardi JA, Chung EM, Chandnani VP, et al. Detection and staging of chondromalacia patellae: relative efficacies of conventional MR imaging, MR arthrography, and CT arthrography. AJR 1994; 163:629–636.
19. Hodler J, Yu JS, Goodwin D, Haghighi P, Trudell D, Resnick D. MR arthrography of the hip: improved imaging of the acetabular labrum with histologic correlation in cadavers. AJR 1995; 165:887–891.
20. Palmer WE, Caslowitz PL, Chew FS. MR arthrography of the shoulder: normal intraarticular structures and common abnormalities. AJR 1995; 164:141–146.
21. Peiss J, Ada G, Casser R, Urhahn R, Günther RW. Gadopentetate-dimeglumine–enhanced MR imaging of osteonecrosis and osteochondritis dissecans of the elbow: initial experience. Skeletal Radiol 1995; 24: 17–20.
22. Murphy BJ. MR imaging of the elbow joint. Radiology 1992; 184:525–529.
23. Chandnani VP, Yeager TD, DeBerardino T, et al. Glenoid labral tears: prospective evaluation with MR imaging, MR arthrography, and CT arthrography. AJR 1993; 161:1229–1235.
24. Engel A. Magnetic resonance knee arthrography. Acta Orthop Scand 1990; 61(Suppl 240):1–57.
25. Siegel S, Castellan NJ Jr. Nonparametric statistics for the behavioral sciences. 2nd ed. New York, NY: McGraw-Hill, 1988.
26. Adam G, Buhne M, Prescher A, Nolte-Ernsting, Bohndorf K, Günther RW. Stability of osteochondral fragments of the femoral condyle: magnetic resonance imaging with histopathologic correlation in an animal model. Skeletal Radiol 1991; 20: 601–606.
27. Gylys-Morin V, Hajek P, Sartoris D, Resnick D. Articular cartilage defects: detectability in cadaver knees with MR. AJR 1987; 148:1153–1157.
28. Hajek P, Baker L, Sartoris D, Neumann C, Resnick D. MR arthrography: anatomic-pathologic investigation. Radiology 1987; 163:141–147.
29. Neumann CH, Petersen SA, Jahnke AH Jr, et al. MRI in the evaluation of patients with suspected instability of the shoulder joint including a comparison with CT-arthrography. ROFO 1991; 154:593–600.
30. Houston CS. Pitfalls to avoid: when is a fabella not a fabella? J Can Assoc Radiol 1978; 29:193.
31. Resnick D. Internal derangements of joints. In: Resnick D, ed. Diagnosis of bone and joint disorders. 3rd ed. Philadelphia, Pa: Saunders, 1995; 2899–3228.
32. Tirman PF, Stauffer AE, Crues JV III, et al. Saline magnetic resonance arthrography in the evaluation of glenohumeral instability. Arthroscopy 1993; 9:550–559.